A Theoretical Investigation of Excited-State Acidity of Phenol and Cyanophenols

Giovanni Granucci,*,† James T. Hynes,‡,§ Philippe Millié,† and Thu-Hoa Tran-Thi†

Contribution from CEA Saclay, DSM/DRECAM/SPAM, Bât. 522, 91191 Gif sur Yvette, France, Department of Chemistry and Biochemistry, University of Colorado, Boulder, Colorado 80309-0215, and Département de Chimie, CNRS UMR 8640, École Normale Supérieure, 24 rue Lhomond, 75231 Paris, France

Received October 18, 1999. Revised Manuscript Received August 28, 2000

Abstract: We present an ab initio study of the first few singlets of the acid/base couples phenol/phenolate and cyanophenols/cyanophenolates in both gas and solution phases. In contrast to the traditional view, the gas-phase calculations indicate that the enhanced acidity of the S_1 state with respect to S_0 arises mainly from effects in the deprotonated species, the effects of excitation on conjugated acids being of minor importance. Evidence for the presence of a conical intersection in the excited state of phenol and *p*-cyanophenol, following the proton dissociation coordinate, has been found, with important consequences for physically realistic reaction geometries in its neighborhood. Solution-phase ab initio calculations on S_0 and S_1 have also been performed, exploiting the polarizable continuum method, and support the conclusions drawn from the gas-phase calculations.

1. Introduction

As is well known, the acidity of hydroxyarene (ArOH) and other conjugated acid molecules is greatly increased upon spectroscopic excitation from the ground electronic state; intermolecular proton transfer from the excited acid to, e.g., a solvent base molecule typically is characterized by a pK_a value some 6 units smaller than for the corresponding ground-state reaction.[1] The enhanced excited-state acidity is, in the standard view, supposed to arise from a partial charge transfer (from the oxygen to the ring) in the excited state of the acid reached upon excitation (the locally excited, LE, state).[2,3] However, the existence of such an intramolecular electronic charge transfer upon excitation has never been directly established, and indeed it has been argued not to occur to any significant extent.[4] In the present paper, this issue will be addressed, with the aid of gas- and solution-phase calculations.

The present paper is the first in a series on the theoretical study of the acid ionization mechanism of electronically excited phenol and cyanophenols in water. The first acid is chosen as the simplest acidic aromatic hydroxyl compound, while the cyanophenols[5] are selected due to the fact that they are much more convenient for ultrafast experimental studies, currently in progress. As is already clear from theoretical studies dealing with the molecular mechanisms of ground-state intermolecular proton-transfer reactions,[6,7] the complete treatment of intermolecular excited-state proton transfer (ESPT) will require attention to a variety of features, including the role of the quantized proton motion, the dynamic involvement of the surrounding solvent molecules, and the electronic rearrangements in the acid−base system associated with the intrinsic proton-transfer act itself. Here we focus on the very first and indispensable step in the theoretical study of the ESPT mechanism in the first excited state, namely the gas-phase characterization of the excited electronic states of the acid/base couples involved in such a process, with a focus on their role in the enhancement of the excited-state acidity. It is to be immediately stressed that since no electronic aspects of the proton-accepting base are addressed in the present work, the electronic issues addressed within are special excited-state electronic aspects present over and above those present in the ground electronic state.[8]

While there have been a number of theoretical studies of phenol and phenolate in the past, the enhanced acidity issues of interest here have not been addressed. Lorentzon et al.[9] have reported an extensive theoretical study of the electronic spectra of phenol, and we will use their work as a point of reference

* To whom correspondence should be addressed. Current address: Dipartimento di Chimica e Chimica Industriale, Università di Pisa, via Risorgimento 35, 56126 Pisa, Italy.

† CEA Saclay.

‡ University of Colorado.

§ École Normale Supérieure.

(1) (a) Förster, T. *Naturwissenschaften* **1949**, *36*, 186. (b) Rosenberg, J. L.; Brinn, I. *J. Phys. Chem.* **1972**, *76*, 3558. (c) Arnaut, L. G.; Formosinho, S. J. *J. Photochem. Photobiol.* **1993**, *75*, 1. (d) Weller, A. *Z. Elektrochem.* **1952**, *56*, 662. (e) Gutman, M.; Nachiel, E. *Biochim. Biophys. Acta* **1990**, *1015*, 391. (f) Jackson, G.; Porter, G. *Proc. R. Soc.* **1961**, *A200*, 13. (g) Mataga, N.; Kubota, T. *Molecular Interactions and Electronic Spectra*; Dekker: New York, 1970; Chapter 7. (h) Syage, J. A. *J. Phys. Chem.* **1995**, *99*, 5772. (i) Douhal, A.; Lahmani, F.; Zewail, A. H. *Chem. Phys.* **1996**, *207*, 477. See also the following special issues: *J. Phys. Chem.* **1991**, *95*, No. 25; *Chem. Phys.* **1989**, *136*, No. 2; *Ber. Bunsen-Ges. Phys. Chem.* **1998**, *102*, No. 3; *Isr. J. Chem.* **1999**, *39*, No. 3−4.

(2) Vander Donckt, E. *Progress in Reaction Kinetics*; Pergamon Press: London, 1970; Vol. 5, p 273.

(3) Salem, L. *Electrons in Chemical Reactions: First Principles*; Wiley: New York, 1982; p 184.

(4) (a) Tran-Thi, T. H.; Prayer, C.; Millié, P.; Uznanski, P.; Hynes, J. T., submitted. (b) Tran-Thi, T. H.; Gustavsson, T.; Prayer, C.; Pommeret, S.; Hynes, J. T. *Chem. Phys. Lett.*, accepted.

(5) Schulman, S. G.; Vincent, W. R.; Underberg, W. J. M. *J. Phys. Chem.* **1981**, *85*, 4068.

(6) (a) Juanós i Timoneda, J.; Hynes, J. T. *J. Phys. Chem.* **1991**, *95*, 10431. (b) Ando, K.; Hynes, J. T. *J. Phys. Chem. B* **1997**, *101*, 10464.

(7) Staib, A.; Hynes, J. T.; Borgis, D. *J. Chem. Phys.* **1995**, *102*, 2487.

(8) The key electronic features of the ground-state acid−base proton-transfer reaction are evidently those in the Mulliken picture (Mulliken, R. S. *J. Chim. Phys.* **1964**, *61*, 20): charge transfer from the nonbonding orbital of the base to the antibonding orbital of the OH bond of the acid; see ref 6 and the following: Ando, K.; Hynes, J. T. *J. Phys. Chem. A* **1999**, *103*, 10398.

(9) Lorentzon, J.; Malmqvist, P. Å.; Fülscher, M.; Roos, B. O. *Theor. Chim. Acta* **1995**, *91*, 91.

10.1021/ja993730j CCC: $19.00
Published on Web 11/23/2000

for the present calculations. For phenolate, the ab initio evaluation of the $S_0 \rightarrow S_1$ transition energy has been carried out,[10,11] but the states were not characterized. To the best of our knowledge, no ab initio calculations on the electronic spectra of cyanophenols and cyanophenolates can be found in the literature.

While the present focus is on gas-phase electronic structure issues, we also present the results of several calculations on the ESPT chemical equilibrium in aqueous solution. In particular, the explicit consideration of equilibrium solvation effects, while not directly related to the ESPT mechanistic details per se, allows us to obtain quantities directly comparable with solution-phase experimental pK_a values. There has been some previous effort along these lines. For example, Monte Carlo simulations were used by Gao et al.[11] to obtain differences in the free energy of solvation yielding the relative (to S_0) excited-state pK_a of phenol. Shüürmann[12] has recently employed COSMO[13]—one version of a number of continuum solvation models available[14]—to obtain the relative ground-state pK_a variation for a series of chlorophenols. In the present work, the equilibrium solvation of ground and excited states of the acid/base couples considered has been obtained with the ab initio continuum solvation PCM method.[15,16] The results are used not only to assess the present calculations in connection with experimental results, but also to provide further insight into the basic issue of the origin of the enhanced excited-state acidity.

The outline of the remainder of this paper is as follows. In section 2, the electronic structure methodology is presented. The results for gas-phase phenol and phenolate ion are presented in section 3, as are those for the cyanophenol acid/base couples. Here we address the issue of the inversion of ^1L_b and ^1L_a states, using Platt notation,[17] which has been an important alternate (and largely orthogonal) theme in previous discussion of ESPT[1g,4,18] (ref 4 can be consulted for an extended discussion on this context). Section 4 deals with various measures of the acidity, both in the gas phase via proton affinity calculations and in solution via estimates of ΔpK_a values. Concluding remarks are offered in section 5.

2. Methods

We have performed ab initio calculations using the double-ζ cc-pVDZ basis set of Dunning.[19] To properly describe the phenolate and cyanophenolate anions, we added a set of s and p diffuse functions on the O and C atoms labeled C_2, C_4, and C_6 in Figure 1, with exponents taken from the aug-cc-pVDZ basis set.[20] For the cyanophenols, diffuse functions were also added on the C and N atoms of the cyano group. Such an arrangement makes it possible (a) to avoid the redundancy problems that arise if diffuse functions are supplied on each carbon atom of the cycle and (b) to span the molecular volume quite uniformly, as is confirmed by the value (0.6) of the overlap between the diffuse s functions on the ring. Note that such a basis set is unsuitable to describe Rydberg states: we are, in fact, mainly interested in aqueous-phase results, where spurious mixing with Rydberg states, that could be a problem in gas-phase calculations, is unlikely. To keep the size of the basis set within reasonable limits for ab initio excited-state calculations, the p polarization functions on the H were discarded (except for the OH hydrogen).

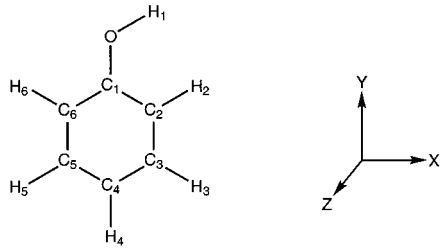

Figure 1. Labeling of atoms and axis convention.

The energies and wave functions for the ground and the two first $\pi\pi^*$ states of phenol and phenolate were obtained with CASSCF calculations. The active space consisted of eight electrons and eight π orbitals: the O p_π, the six ring π, and one extravalence π orbital, this last added in order to have a balanced description for phenol and phenolate. This resulted in 4900 determinants in the A′ irreducible representation (the C_s symmetry was used throughout). Similar CASSCF calculations were also performed for the cyano derivatives: in this case, the active space contained two more electrons and two more π orbitals (from the cyano group), resulting in 63504 determinants. The presence of charge-transfer character in an excited state can introduce a considerable repolarization of the σ system with respect to the ground state. As one of our aims is to assess the presence of an intramolecular charge transfer in S_1, we have to correctly take into account the repolarization of the σ system. Therefore, in our CASSCF calculations, the orbitals were optimized separately for each electronic state (such calculations will be called hereafter "state-to-state CASSCF"). Unfortunately, due to convergence problems, in most cases it was not possible to obtain S_2 with state-to-state CASSCF calculations. For this reason we have performed state-averaged CASSCF calculations, and the repolarization of the σ system, together with the dynamical correlation, has been taken into account with the aid of the CASPT2[21] perturbative method, as implemented in the MOLCAS[22] program package. Electrostatic properties and oscillator strengths have been obtained with the CASSCF wave functions.

The quantity W_{PT2}, which is reported in the tables, is the weight of the reference wave function in a perturbative calculation, i.e., the norm of the reference wave function when the total perturbed wave function is normalized to 1. Such a quantity is an important indicator for a perturbative calculation and should not be very far from 1, since otherwise the supposed perturbation is not very small and the result is not trustworthy. The norm of the perturbative correction,[25] N_{PT2} of the (normalized) reference wave function is connected to W_{PT2} by the following simple relation: $N_{PT2} = (1 - W_{PT2})/W_{PT2}$.

In the case of phenolate anion, CIPSI[23,24] calculations were also performed. The molecular orbitals were the state-averaged CASSCF natural orbitals and the final S space, containing 22 399 determinants, was the union of two subspaces of configurations: (1) the CAS space and (2) a space generated starting from the first few configurations contributing the most to the states considered and then selecting in the perturbative space with a threshold $\sigma = 0.2$. We have used a selection

(10) Krauss, M.; Jensen, J. O.; Hameka, H. F. *J. Phys. Chem.* **1995**, *98*, 9955.
(11) Gao, J.; Li, N.; Freindorf, M. *J. Am. Chem. Soc.* **1996**, *118*, 4912.
(12) Shüürmann, G. *J. Chem. Phys.* **1998**, *109*, 9523.
(13) (a) Klamt, A.; Schüürmann, G. *J. Chem. Soc., Perkins Trans. 2* **1993**, 799. (b) Klamt, A.; Jonas, V. *J. Chem. Phys.* **1996**, *105*, 9972.
(14) Tomasi, J.; Persico, M. *Chem. Rev.* **1994**, *94*, 2027.
(15) Mennucci, B.; Cammi, R.; Tomasi, J. *J. Chem. Phys.* **1998**, *109*, 2798.
(16) Amovilli, C.; Barone, V.; Cammi, R.; Cancès, E.; Cossi, M.; Mennucci, B.; Pomelli, C. S.; Tomasi, J. *Adv. Quantum Chem.* **1999**, *32*, 227.
(17) Platt, J. R. *J. Chem. Phys.* **1949**, *17*, 484.
(18) (a) Tramer, A.; Zaborowska, M. *Acta Phys. Polon.* **1968**, *34*, 821. (b) Knochenmuss, R. D.; Smith, D. E. *J. Chem. Phys.* **1994**, *101*, 7327. (c) Knochenmuss, R. D.; Muiño, P. L.; Wickleder, C. *J. Phys. Chem.* **1996**, *100*, 11218. (d) Tolbert, L. M.; Haubrich, J. E. *J. Am. Chem. Soc.* **1990**, *112*, 8163. (e) Tolbert, L. M.; Haubrich, J. E. *J. Am. Chem. Soc.* **1994**, *116*, 10593.
(19) Dunning, T. H., Jr. *J. Chem. Phys.* **1989**, *90*, 1007.
(20) Kendall, R. A.; Dunning, T. H., Jr.; Harrison, R. J. *J. Chem. Phys.* **1992**, *96*, 6769.
(21) Andersson, K.; Malmqvist, P. Å.; Roos, B. O. *J. Chem. Phys.* **1992**, *96*, 1218.
(22) Andersson, K.; Blomberg, M. R. A.; Fülscher, M. P.; Karlström, G.; Lindh, R.; Malmqvist, P. Å.; Neogrády, P.; Olsen, J.; Roos, B. O.; Sadlej, A. J.; Schütz, M.; Seijo, L.; Serrano-Andrés, L.; Siegbahn, P. E. M.; Widmark, P. O. *MOLCAS*, Version 4.1; Lund University, Sweden, 1997.
(23) Huron, B.; Malrieu, J. P.; Rancurel, P. *J. Chem. Phys.* **1973**, *58*, 5745.
(24) Cimiraglia, R. *Int. J. Quantum Chem.* **1996**, *60*, 167.
(25) Angeli, C.; Persico, M. *Theor. Chem. Acc.* **1997**, *98*, 117.

Table 1. Bond Lengths (Å) and Bond Angles for S_0, S_1, and S_2 of Phenol[a]

	S_0		S_1		S_2
	CAS	exp[30]	CAS	exp[32]	CAS
C_1-C_2	1.3942	1.3912	1.4327	1.445	1.3748
C_2-C_3	1.4002	1.3944	1.4338	1.442	1.4834
C_3-C_4	1.3943	1.3954	1.4355	1.445	1.5057
C_4-C_5	1.4006	1.3954	1.4344	1.445	1.3839
C_5-C_6	1.3937	1.3922	1.4362	1.443	1.4834
C_6-C_1	1.3994	1.3912	1.4286	1.445	1.4763
C_2-H_2	1.0854	1.0856	1.0828		1.0825
C_3-H_3	1.0832	1.0835	1.0807		1.0793
C_4-H_4	1.0828	1.0802	1.0820		1.0800
C_5-H_5	1.0833	1.0836	1.0807		1.0825
C_6-H_6	1.0823	1.0813	1.0799		1.0773
C−O	1.3549	1.3745	1.3492	1.2565	1.3340
O−H	0.9450	0.9574	0.9458		0.9483
$C_1-C_2-C_3$	119.96	119.43	119.00		118.71
$C_2-C_3-C_4$	120.39	120.48	119.68		120.15
$C_3-C_4-C_5$	119.32	119.24	120.83		119.06
$C_4-C_5-C_6$	120.57	120.79	119.67		121.36
$C_5-C_6-C_1$	119.82	119.22	119.01		117.77
$C_6-C_1-C_2$	119.95	120.85	120.81		122.96
$C_1-C_2-H_2$	120.02	120.01	120.27		121.08
$C_2-C_3-H_3$	119.38	119.48	120.12		119.83
$C_3-C_4-H_4$	120.37	120.25	119.49		119.66
$C_4-C_5-H_5$	120.01	119.78	120.13		120.65
$C_5-C_6-H_6$	121.38	121.55	121.96		122.66
C_6-C_1-O	117.39	117.01	116.77		113.04
C_1-O-H_1	110.28	108.77	110.34		120.26

[a] See Figure 1 for the labeling of the atoms.

procedure recently put forward by Angeli and Persico,[25] which allows one to choose (approximately) the norm of the perturbative correction, represented by the σ threshold, of a subsequent perturbative calculation with the selected configurations. The Epstein−Nesbet partition of the Hamiltonian[26] was used. Electrostatic properties and oscillator strengths were obtained at the variational level.

The solution-phase calculations to be discussed in sections 4.2 and 4.3 were carried out with the PCM method,[15,16] in the version implemented in the GAMESS[27] quantum chemistry package. In particular, state-to-state CASSCF calculation were performed, using the same active spaces described above. For comparative purposes, the gas-phase proton affinities (section 4.1) were also obtained with state-to-state CASSCF calculations. Full equilibrium solvation was considered for all the states.

Geometry optimizations at RHF/cc-pVDZ level were performed for all the species here considered. For phenol, S_0, S_1, and S_2 states were also optimized by state-to-state CASSCF calculations, with the cc-pVDZ basis set. Acidity calculations (section 4) have been performed with all the species at their RHF/cc-pVDZ-optimized geometry.

3. Gas-Phase Calculations

3.1 Phenol. In Table 1 are shown the bond lengths and bond angles optimized for the S_0, S_1, and S_2 states of phenol at the CASSCF level, using the cc-pVDZ basis set, in the C_s symmetry of the ground state.[28] Our results are in agreement with the CASSCF, DFT, and CIS optimization of Schumm et al.[29] for the S_0 and S_1 states of phenol; the S_2 optimized geometry has not been previously reported. The experimental geometry of S_0 has been determined by Larsen[30] from microwave spectroscopy of a set of six isotopomers. Portalone et al.[31] have obtained structural parameters quite close to those of Larsen by electron diffraction experiments. Our calculated ground-state geometry is in overall good agreement with the experimental one, with variations up to 0.02 Å for the bond lengths and up to 0.9° for the bond angles. The C−O and O−H bond lengths follow the expected trend, since the σ system is uncorrelated. For S_1, we found a lengthening of the C−C bonds of about 0.03−0.04 Å with respect to the ground state, while the C−O and O−H bonds are almost unaffected. Berden et al.[32] estimate a shortening by 0.12 Å of the C−O bond upon excitation from the excited-state rotational constants obtained by high-resolution UV spectroscopy. Such an interpretation is based on the assumption that the stronger acidity of the phenol S_1 state with respect to the ground state should imply a shortening of the C−O bond, due to an enhanced interaction between the oxygen lone pair and the π electrons of the ring.[33] In our calculation, both the shortening of the C−O bond and the charge transfer from the oxygen to the ring are negligible in PhOH (see below), suggesting that the increase in acidity should result from a different effect.

For S_2, we found a quite different geometry with respect to the ground state, showing the largest variation (up to 0.11 Å) for the C−C bond lengths and for the C_1-O-H_1 bond angle. In particular, even if three long and two short C−C bonds can be distinguished, the structure obtained, with localized double bonds, is not that expected from charge transfer from the oxygen atom to the ring (for example, the quinoidal structure found for the ground state of phenolate; see the next section). However, the non-negligible shortening of the C−O bond length (0.02 Å with respect to the ground state) indicates that a non-negligible charge-transfer contribution should be present in the S_2 state, in agreement with the dipole moment pattern (see below).

In Tables 2 and 3 are shown the features of the three singlet states of phenol considered here. To ease the subsequent

Table 2. Phenol Transition Energies (eV)[a]

		vertical			adiabatic			exp
state		CAS	PT2	W_{PT2}	CAS	PT2	W_{PT2}	0−0
$\tilde{X}$		0	0	0.77	0	0	0.76	0
"$^1B_1$"	^1L_b	4.877	4.643	0.66	4.737[b]	4.364[b]	0.75	4.507[c]
"$^1A_1$"	^1L_a	7.660	6.264[e]	0.60	7.246	6.394[e]	0.75	5.77[d]

[a] W_{PT2} is the weight of the CAS reference in the perturbative calculations. [b] Taking into account the ZPE variation, calculated to be 0.148 eV by Schumm et al.[29], we found 4.589 and 4.216 eV for the CASSCF and CASPT2 transition energies, respectively. [c] From refs 32 and 34. [d] From ref 35. [e] The incongruence between "vertical" and "adiabatic" CASPT2 results for S_2 is due to the fact that geometry optimizations have been done at the CASSCF level.

Table 3. Phenol Singlet States: Properties from State-Averaged CASSCF Calculations

		dipole (au)[a]			f[b]	
state		x	y	$\langle z^2 \rangle$ (au)	calc	exp[35]
$\tilde{X}$		0.56	−0.19	34.1		
"$^1B_1$"	^1L_b	0.61	−0.19	33.9	0.007 (−15)	0.020
"$^1B_1$"	^1L_a	0.31	0.76	34.1	0.045 (55)	0.132

[a] 1 au = 2.542 D. [b] Dipole oscillator strength; in parentheses is given the angle of the transition dipole moment with the x direction (see Figure 1).

(26) (a) Epstein, P. S. *Phys. Rev.* **1926**, *28*, 695. (b) Nesbet, R. K. *Proc. R. Soc. London Ser. A* **1955**, *230*, 312.

(27) Schmidt, M. W.; Baldridge, K. K.; Boatz, J. A.; Elbert, S. T.; Gordon, M. S.; Jensen, J. J.; Koseki, S.; Matsunaga, N.; Nguyen, K. A.; Su, S.; Windus, T. L.; Dupuis, M.; Montgomery, J. A. *J. Comput. Chem.* **1993**, *14*, 1347.

(28) Keresztury, G.; Billes, F.; Kubinyi, M.; Sundius, T. *J. Phys. Chem.* **1998**, *102*, 1371.

(29) Schumm, S.; Gerhards, M.; Roth, W.; Gier, H.; Kleinermanns, K. *Chem. Phys. Lett.* **1996**, *263*, 126.

(30) Larsen, N. W. *J. Mol. Struct.* **1979**, *51*, 175.

(31) Portalone, G.; Shultz, G.; Dominicano, A.; Hargittai, I. *Chem. Phys. Lett.* **1992**, *197*, 482.

(32) Berden, G.; Meerts, W. L.; Schmitt, M.; Kleinermanns, K. *J. Chem. Phys.* **1996**, *104*, 972.

(33) Martinez, S. J., III; Alfano, J. C.; Levy, D. H. *J. Mol. Spectrosc.* **1992**, *152*, 80.

comparison with the phenolate anion, the states have been (approximately) classified in the irreducible representations of the C_{2v} symmetry group. The Platt[17] notation has also been used: the first two excited valence singlets are labeled as ^1L_b and ^1L_a, which means that their dipole transition moment is, respectively, approximately perpendicular and parallel to the C−O axis. Experimentally, the lowest singlet is well characterized and known to be a b-type band (i.e., with the transition dipole in the *x* direction;[32] see Figure 1) with a band origin at 4.507 eV[32,34] and an absorption maximum at 4.59 eV.[35] We have obtained the vertical excitation energies from a state-averaged CASSCF calculation at the S_0 optimized geometry and the adiabatic energies from state-to-state CASSCF calculations. Taking into account the zero-point energy (ZPE) difference between S_0 and S_1, which has been calculated by Schumm et al.[29] to be 1193 cm^{-1}, we find 4.589 eV for the adiabatic transition at the CASSCF level, in very good accord with the experimental value, while the perturbative calculation gives a ZPE-corrected transition energy that is too low by 0.291 eV. From Table 2 we obtain a difference between the vertical and the adiabatic $S_0 \rightarrow S_1$ CASSCF transition energy of 0.15 eV, which is in reasonable agreement with the experimental difference (0.08 eV) between the absorption maximum and the band origin. The CASPT2 difference, 0.37 eV, is too high; note, however, that the geometry optimizations were done at the CASSCF level.

As one can see from Table 3, the phenol dipole moment is almost unchanged upon electronic excitation to S_1, in agreement with previous calculations.[9,10] Hence, we expect charge transfer from the oxygen to the ring to have negligible contribution in S_1, in contrast with the standard explanation for the enhanced excited-state acidity.[2,3] This is also confirmed by the variation of the Löwdin charges on the oxygen atom upon excitation: on passing from S_0 to S_1, the Löwdin charge on the hydroxyl group decreases by only 0.025 au, while for S_2 the decrement is 0.093 au (from state-averaged CASSCF calculations; very similar results are obtained at the CASPT2 level). Even though care must be taken with Löwdin charges, especially when the basis set contains diffuse functions, we expect the difference of Löwdin charges to be meaningful. To the best of our knowledge, the inconsistency of the calculated electrostatic properties of S_1 with the standard explanation for its enhanced acidity has not been pointed out before.

Not much is known about the S_2 band of phenol; Kimura and Nagakura[35] found 5.82 for the vertical transition, and the band origin can be estimated to be at 5.77 eV (see Lorentzon et al.[9]). While the $S_0 \rightarrow S_2$ transition energy obtained with the CASSCF calculations greatly exceeds the experimental value, the perturbative treatment is effective in reducing the difference between the calculated and the experimental values (cf. Table 2). Such behavior has already been reported by Lorentzon et al.[9] and is most probably due to an underestimation of the weight of ionic configurations in the S_2 state at the CASSCF level, due to the lack of dynamical correlation. The difference in the value of the dipole moment between S_0 and S_2 and in the value of the Löwdin charge on the oxygen atom (see above) indicates that S_2 has an appreciable charge-transfer character (from the oxygen to the ring), and therefore ionic configurations should have a non-negligible weight in S_2. From Table 3, the calculated ratio of the oscillator strengths for the S_2 and S_1 transitions is 6.4, in very good agreement with the experimental result (6.6). As is evident from the $\langle z^2 \rangle$ values, the two valence excited states considered here show no relevant mixing with Rydberg states, in agreement with the results of ref 9.

Table 4. Bond Lengths and Bond Angles at the RHF/cc-pVDZ Level for the Phenolate Anion[a]

bond lengths (Å)		bond angles (deg)	
C_1-C_2	1.443	$C_1-C_2-C_3$	122.64
C_2-C_3	1.378	$C_2-C_3-C_4$	122.20
C_3-C_4	1.398	$C_1-C_2-H_2$	116.87
C−O	1.244	$C_2-C_3-H_3$	118.68
C_2-H_2	1.085		
C_3-H_3	1.088		
C_4-H_4	1.084		

[a] See Figure 1 for the labeling of the atoms.

Let us summarize the main results of this section: (a) The S_1 (^1L_b) state of phenol is characterized by a charge distribution very similar to that of the ground state, and this is incompatible with the standard view for the enhanced acidity of S_1. (b) In the S_2 (^1L_a) state of phenol, a non-negligible charge transfer from the oxygen to the ring is apparent.

3.2. Phenolate. The geometrical parameters of the phenolate anion used in the calculations have been obtained with RHF/cc-pVDZ optimization and are shown in Table 4. C_{2v} symmetry has been imposed. Note that the phenolate has a quinoidal structure: one can recognize a pattern with three "short" bonds (C−O, and the two C−C bonds parallel to the C−O axis) and four "long" C−C bonds. Such an observation suggests that the oxygen atom is involved in a resonance phenomenon with the ring, in which delocalization of the negative charge from the oxygen to the ring occurs. In particular, the C−O bond length (1.24 Å) indicates a non-negligible double bond character for the C−O bond, in agreement with the findings of Suter and Nonella for the ground-state anion.[36]

The calculations are complicated by the fact that the gas-phase valence excited states of phenolate are autoionizing. It is experimentally known from UV photoelectron spectroscopy[37] that the adiabatic ionization potential of the phenolate anion in the gas phase is 2.253 eV. Evidence for an autoionizing state at about 3.5 eV has been found in the photoelectron experiments.[37] Such a value compares quite well with the findings of Richardson et al.,[38] who have obtained a photodetachment spectrum of gaseous phenolate which shows a maximum at 340 nm (3.65 eV), attributed to the autoionizing state. We have calculated the phenolate ionization potential at the CASSCF and CASPT2 levels, using also for phenoxyl radical the RHF/cc-pVDZ-optimized geometry. The results are, respectively, 1.270 and 1.977 eV and follow the expected trend, because of the difference of correlation energy in the two species.[39] The good agreement between the CASPT2 and experimental (2.253 eV) ionization potentials confirms the validity of the basis set we have chosen, at least for the ground state of phenolate.

We have found no evidence for excited valence singlets below the ionization threshold: S_1 and S_2 considered here are autoionizing states. They belong to the A_1 and B_1 irreducible representations of the C_{2v} symmetry group and can be labeled, in Platt notation, as ^1L_a and ^1L_b (respectively for $^1A_1$ and $^1B_1$). Just as for phenol, ^1L_a and ^1L_b are characterized by a dipole transition moment respectively parallel and perpendicular to the

(34) Bist, H. D.; Brand, J. C. D.; Williams, D. R. *J. Mol. Spectrosc.* **1967**, *24*, 413.

(35) Kimura, K.; Nagakura, S. *Mol. Phys.* **1965**, *9*, 117.

(36) Suter, H. U.; Nonella, M. *J. Phys. Chem. A* **1998**, *102*, 10128.

(37) Gunion, R. F.; Gilles, M. K.; Polak, M. L.; Lineberger, W. C. *Int. J. Mass Spectrom. Ion Processes* **1992**, *117*, 601.

(38) Richardson, J. H.; Stephenson, L. M.; Brauman, J. I. *J. Am. Chem. Soc.* **1975**, *97*, 2967.

(39) Note, in fact, that on going from phenol to phenoxyl an electron pair is broken; such a pair is markedly more correlated at the CASPT2 level than by our CASSCF calculations.

Table 5. Phenolate Singlet States: Transition Energies (eV) and Properties[a]

state		CAS	PT2	W_{PT2}	μ_y	$\langle z^2 \rangle$	f
$\tilde{X}$	$^1A_1$	0	0	0.75	−1.93	36.0	
$^1A_1$	^1L_a	3.857	4.403	0.75	0.37	56.1	0.090
$^1B_1$	^1L_b	4.184	4.382	0.74	−2.23	47.0	0.292

[a] W_{PT2} is the weight of the CAS reference in the perturbative calculations, μ is the dipole moment (with respect to the center of the nuclear charges), and f is the dipole oscillator strength. μ_y and $\langle z^2 \rangle$ in au (1 au = 2.542 D).

Table 6. Phenolate Singlet States: CIPSI Results[a]

state		CIPSI-EN	W_{PT2}	μ_y	$\langle z^2 \rangle$	f
$\tilde{X}$	$^1A_1$	0	0.84	−1.93	36.1	
$^1A_1$	^1L_a	4.513	0.83	0.40	56.5	0.036
$^1B_1$	^1L_b	4.568	0.83	−2.10	46.5	0.139

[a] The Epstein−Nesbet partition of the Hamiltonian is used. For the meaning of labels, see Table 5.

C−O axis. The results of our calculations for the phenolate anion in the gas phase are shown in Tables 5 and 6. As one can see from the value of the dipole moment (which is calculated with respect to the center of the nuclear charges), S_0 and $^1B_1$ are characterized by a similar charge distribution, which strongly differs from the $^1A_1$ charge distribution. In particular, a non-negligible contribution of charge-transfer character from the oxygen to the ring is present in the $^1A_1$ state: considering the variation of the dipole moment between $^1A_1$ and S_0 (2.3 au, both at the CASSCF and at the CIPSI level), one can roughly estimate that a negative charge of 0.45 *e* is transferred from the oxygen to the ring center upon the $S_0 \rightarrow {}^1A_1$ transition.

It is apparent from Tables 5 and 6 that the first two excited $\pi \rightarrow \pi^*$ singlets are quite close in energy and that with our CASSCF and CASPT2 calculations their energetic order cannot be established unambiguously. In an attempt to clarify the issue, we have also performed CIPSI calculations, characterized by bigger values of the reference weight with respect to CASPT2 calculations. The energetic order of $^1A_1$ and $^1B_1$ at the CIPSI level coincides with the CASSCF one, although the energy difference between the two excited states is only 0.06 eV[40].

Further information can be obtained by consideration of the oscillator strengths for the $S_0 \rightarrow {}^1B_1$ and the $S_0 \rightarrow {}^1A_1$ transitions, which are in a ratio of 3.2 at the CASSCF and 3.8 at the CIPSI levels. Experimentally,[41] the first two peaks in the phenolate UV absorption spectrum in aqueous solution are found at 4.32 and 5.30 eV, with comparable fwhm and maximum value of the molar extinction coefficient respectively equal to 2560 and 9690. Therefore, if one assumes that the oscillator strengths of the two transitions considered have similar values in the gas phase and in solution, the energetic order of the first two valence excited singlets of phenolate should be $^1A_1$ and $^1B_1$ (i.e., the one obtained in the CASSCF and CIPSI calculation), at least in aqueous solution. Note, moreover, that the CASSCF result for $S_0 \rightarrow S_1$ transition energy shows better agreement with the experimental value of 3.5−3.65 eV. In approximate Platt language, the evident order of the phenolate excited states is ^1L_a and ^1L_b, inverted with respect to the phenol excited states.

(40) As can be checked from the $\langle z^2 \rangle$ values, $^1A_1$ shows non-negligible mixing with Rydberg states, and it is therefore more sensitive than $^1B_1$ to the presence of diffuse functions in the basis set. In fact, deleting them has the effect of raising the transition energy of $^1A_1$ at each level of calculation considered here, while the transition energy of $^1B_1$ is almost unaffected (adding diffuse functions on each atomic center yields results comparable to those shown in Tables 5 and 6).

(41) Herington, E. F. G.; Kynaston, W. *Trans. Faraday Soc.* **1957**, *53*, 238.

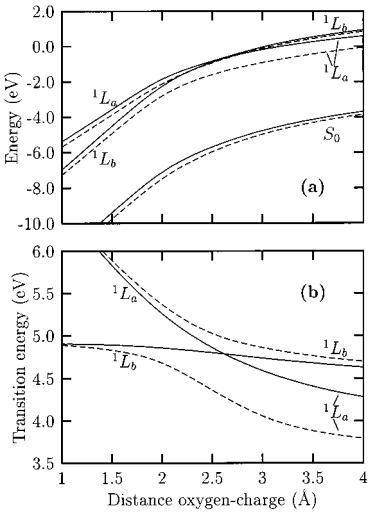

Figure 2. Interaction between the phenolate anion and the proton, modeled as a unit positive charge. Full lines: the charge is approached on the C−O axis. Dashed lines: the charge is approached following the O−H direction in phenol. (a) S_0, ^1L_a, and ^1L_b energies with respect to the ground state of phenolate alone. (b) ^1L_a and ^1L_b transition energies.

The qualitative behavior of the two diabatic states ^1L_a and ^1L_b along the $PhO^- \cdots H^+$ proton dissociation coordinate can be easily understood in terms of electrostatic interactions when the O−H distance becomes sufficiently large. As one can see from the dipole moments (see Table 3), in the approach of a positive charge to the phenolate anion, the transition energy of ^1L_b will remain approximatively constant due to the small difference in ground- and excited-state dipole moments, while the ^1L_a transition energy will rise, due to the charge transfer in the anion reducing the negative charge on O. Therefore, in the proton dissociation process from phenol to phenolate, at least for O−H distances sufficiently large for the electrostatic interactions to become dominant, we expect the ^1L_a transition energy to decrease and approach ^1L_b, or possibly cross it as in our CASSCF calculations. Our calculations do not permit the unambiguous establishment of the presence of the crossing, so caution is necessary here, even if the pattern of the oscillator strengths is in accord with the presence of the crossing (see above). Note that the crossing is permitted in a C_{2v} arrangement (C−O−H collinear) in which ^1L_a and ^1L_b belong to different irreducible representations (respectively $^1A_1$ and $^1B_1$), but it is avoided in C_s symmetry, yielding therefore a conical intersection[42] in the excited state of phenol along the proton dissociation coordinate, the center of the intersection being on the C−O axis (other geometries are considered below). This is shown in Figure 2, where we report the variation of the ^1L_a and ^1L_b transition energies, calculated at the CASSCF level, when a positive charge is approached to the phenolate anion. We are unaware of any previous explicit discussion of conical intersection in the proton-transfer context in the literature.

The center of the conical intersection appears to be located at a distance of about 2.6 Å from the oxygen atom, on the C−O axis. This $O-H^+$ distance is certainly larger than the equilibrium bond length in phenol (about 0.95 Å, see Table 1) and is even comparable to the estimated O−O separation in the complex

(42) (a) Michl, J.; Bonačić-Koutecký, V. *Electronic Aspects of Organic Photochemistry*; Wiley: New York, 1990. (b) Klessinger, M. *Angew. Chem., Int. Ed. Engl.* **1995**, *34*, 549. (c) Sobolewski, A. L.; Woywod, C.; Domcke, W. *J. Chem. Phys.* **1993**, *98*, 5627. (d) Garavelli, M.; Bernardi, F.; Olivucci, M.; Vreven, T.; Klein, S.; Celani, P.; Robb, M. A. *Faraday Discuss.* **1998**, *110*, 51. (e) Cattaneo, P.; Granucci, G.; Persico, M. *J. Phys. Chem. A* **1999**, *103*, 3364.

Table 7. Optimized C−O Bond Lengths (in Å) at the RHF/cc-pVDZ Level

molecule	C−O	molecule	C−O
PhOH	1.351	PhO^-	1.244
o-CP	1.337	*o*-CP^-	1.230
m-CP	1.347	*m*-CP^-	1.238
p-CP	1.342	*p*-CP^-	1.234

$PhOH-H_2O$ (the experimentally evaluated[32] O−O distance from the phenol O to the hydrogen bonded water molecule in the gas phase is itself 2.93 Å); it is likely to be comparable with or even larger than the equilibrium O−O distance in a phenolate−hydronium ion cluster, if such a cluster exists. However, in our CASSCF calculations, the $S_0 \rightarrow S_2$ transition energy is overestimated by about 2 eV, which, since it positions the acid S_2 state at too high a value, leads to a serious overestimation of the oxygen−proton distance at which the center of the conical intersection occurs. While this feature needs to be further examined in the presence of a proton-accepting base molecule (and further surrounding solvent molecules), it seems that the presence of the conical intersection could play an important role in the dynamics of the excited-state proton-transfer reaction. In fact, even though the center of the conical intersection is situated on a physically unlikely C−O axis approach, the related induced avoided crossing is still clearly identifiable on the physically realistic O−H axis approach, as one can see from Figures 2 and 3. The connection of the excited-state inversion between the acid and anion species to earlier views for ESPT[2,3] will be discussed in the concluding section 5.

3.3. Cyanophenols and Cyanophenolates. The results for *o*-, *m*-, and *p*-cyanophenols are shown in Table 8. In all cases, the RHF/cc-pVDZ-optimized geometries were used. The optimized C−O bond lengths are shown in the left part of Table 7. A pattern rationalizable in terms of inductive and mesomeric effects is apparent: in fact, the cyano group has an inductive (electron-withdrawing) and a mesomeric effect (in ortho and para positions), both assisting in shortening the C−O bond.[43] All three isomers are found to belong to the C_s symmetry group. The excited $\pi \rightarrow \pi^*$ singlet states we have considered can therefore be classified as $^1A'$ as for phenol. The orientation of Figure 1 is retained. In the case of *o*-cyanophenol (*o*-CP), only the most stable of the two rotational isomers (which forms an intramolecular hydrogen bond) was considered.

Our calculated transition energies for the acids compare quite well with the available experimental results, especially at the CASPT2 level of computation. In particular, the $S_0 \rightarrow S_1$ transition energy is overestimated by 0.615 (15%) and 0.422 (9%) eV for respectively *o*- and *p*-CP at the CASSCF level and only by 0.163 (4%) and 0.071 (2%) eV at the CASPT2 level. These errors should be, at least in part, attributed to the fact that we are comparing vertical with experimental adiabatic transition energies, and to the differential ZPE correction. Note, in fact, that the CASPT2 errors are quite close to the experimental difference between vertical and adiabatic transition in phenol, which is 0.08 eV.

Note in Table 8 that the reference weight in the perturbative calculations for the case of the S_1 and S_2 states of *o*-CP is exceedingly small (it corresponds to a norm of the perturbative correction of the reference wave function of 1.33 and 3.17 for S_1 and S_2, respectively); this is due to the interaction with intruder states, built on diffuse orbitals, which have a small interaction matrix element but are close in energy to the state to be perturbed. However, it is important to appreciate that this produces a large perturbative correction only for the wave function; in our case, for the S_2 state of *o*-CP there is a configuration that contributes to the first-order perturbation of the wave function with a coefficient of 1.64 and that gives a contribution to the second-order energy correction of only 0.007 au (i.e., 0.6% of the total energy correction). We can therefore reasonably expect still meaningful results for the transition energy at the CASPT2 level, which is confirmed by the agreement with the available experimental results indicated in Table 8. To further clarify this point, we have also performed a CASPT2 calculation for *o*-CP excluding the diffuse functions from the basis set; the results closely match those shown in Table 8, except that the references weights are now reasonable (between 0.70 and 0.72), thus validating our findings with the full basis set.

On the basis of the values of the dipole moments, the considerations stated in section 3.1 for phenol can be implemented for the three CP isomers: the electronic charge distribution does not seem to vary appreciably for S_1, while a marked variation is produced for S_2. Specifically, it can be seen from a Löwdin population analysis that, going from S_0 to S_2, electron density is gained by the cyano group while the OH is depleted; for instance, for *p*-CP the charge variation is 0.11 *e* on OH and −0.04 *e* on CN, while on going from S_0 to S_1 the charge variation is only 0.01 *e* for both OH and CN. The other isomers show a similar pattern: for both *o*-CP and *m*-CP, the Löwdin charge variation from S_0 to S_2 is 0.07 *e* for OH and −0.09 *e* for CN (0.03 *e* for OH and −0.03 *e* for CN from S_0 to S_1). This behavior is confirmed by the variation of the dipole moment for the para isomer. For the *o*- and *m*-CP, the charge-transfer contribution cannot be, for symmetry reasons, easily identified from the variation of the dipole moment. However, the Löwdin charge variation pattern shown above indicates that the S_1 and S_2 charge distributions of the ortho and meta isomers follow a similar pattern with respect to the phenol and *p*-CP; in particular, the S_2 state appears to have a non-negligible charge-transfer contribution from the oxygen, while the S_1 charge distribution is more similar to the ground-state one. This conclusion is confirmed by experimental results[44] concerning the S_1 state of *o*-CP.

Turning to the anions, the results for the three cyanophenolate isomers are summarized in Table 9. Just as was done for the cyanophenols, the geometries were optimized at the RHF/cc-pVDZ level. The optimized C−O bond lengths are shown on the right part of Table 7 and follow the same pattern remarked above for cyanophenols. The *p*-cyanophenolate (*p*-CP^-) isomer belongs to the C_{2v} symmetry group, and therefore the same considerations reported in section 3.2 for the phenolate anion apply also to *p*-CP^-; in particular, an inversion of the excited states between the acid and the anion occurs (Tables 8 and 9), and there is charge transfer from the oxygen in the $^1A_1$ state. Indeed, concerning the first point, in our CASSCF calculations a conical intersection following the proton dissociation coordinate is apparent. The behavior of the ^1L_a and ^1L_b states of *p*-CP^- following the proton dissociation coordinate has been modeled by approaching a positive charge (just as was done for phenolate) and is shown in Figure 3. The center of the conical intersection appears to be located at an $O-H^+$ distance of about 3.5 Å on the C−O axis; on the basis of the results obtained for phenol (see section 3.2), we expect such a distance to be overestimated.

Concerning the second point about the charge distribution

(43) (a) Taft, R. W.; Lewis, I. C. *J. Am. Chem. Soc.* **1958**, *80*, 2436. (b) Taft, R. W.; Lewis, I. C. *J. Am. Chem. Soc.* **1960**, *81*, 5343.

(44) Ram, S.; Yadav, J. S.; Bist, H. D. *Prāmana* **1984**, *22*, 17.

Table 8. Cyanophenols Singlet States: Gas-Phase Results[a]

		transition energy (eV)				dipole (au)			
molecule	state	CAS	PT2	exp	W_{PT2}	μ_x	μ_y	$\langle z^2 \rangle$	f[d]
o-CP	S_0	0	0	0	0.72	−1.00	−0.95	43.4	
	S_1	4.825	4.373	4.210[b]	0.43	−0.99	−0.96	45.0	0.024 (−25)
	S_2	7.322	5.837		0.24	−1.62	−0.77	45.1	0.263 (4)
m-CP	S_0	0	0	0	0.72	−0.93	0.82	40.6	
	S_1	4.803	4.452		0.68	−0.90	0.87	40.7	0.018 (21)
	S_2	7.106	5.958		0.69	−1.56	1.69	41.6	0.164 (−13)
p-CP	S_0 "$^1A_1$"	0	0	0	0.72	0.66	1.73	40.7	
	S_1 "$^1B_1$"	4.929	4.578	4.507[c]	0.71	0.67	1.54	40.5	0.001 (−4)
	S_2 "$^1A_1$"	7.012	5.396		0.69	0.71	3.52	41.0	0.411 (86)

[a] For the meaning of labels see Table 5. [b] References 44 and 59 (0−0 band). [c] Reference 60 (0−0 band). [d] In parentheses is given the angle of the transition dipole moment with the *x* direction.

Table 9. Cyanophenolates Singlet States: Gas-Phase Results[a]

		transition energy (eV)			dipole (au)			
molecule	state	CAS	PT2	W_{PT2}	μ_x	μ_y	$\langle z^2 \rangle$	f[b]
o-CP^-	S_0	0	0	0.71	−1.15	−2.13	42.5	
	S_1	4.077	4.470	0.69	−0.31	−0.41	61.2	0.050 (−35)
	S_2	4.113	3.578	0.66	−1.12	−1.50	45.7	0.223 (11)
m-CP^-	S_0	0	0	0.71	−0.77	−1.33	42.5	
	S_1	3.957	3.454	0.62	−1.28	−0.40	46.1	0.139 (11)
	S_2	4.090	4.465	0.65	−0.66	0.55	61.0	0.042 (−48)
p-CP^-	$S_0\ ^1A_1$	0	0	0.71	0	−0.30	42.6	
	$S_1\ ^1A_1$	4.004	4.697	0.70	0	0.76	65.1	0.003 (90)
	$S_2\ ^1B_1$	4.219	4.420	0.70	0	−0.98	50.0	0.137 (0)

[a] For the meaning of labels see Table 5. [b] In parentheses is given the angle of the transition dipole moment with the *x* direction.

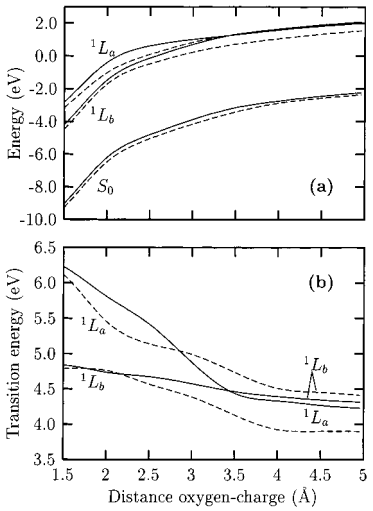

Figure 3. Interaction between the *p*-cyanophenolate anion and the proton, modeled as a unit positive charge. Full lines: the charge is approached on the C−O axis. Dashed lines: the charge is approached following the O−H direction in *p*-CP. (a) S_0, ^1L_a, and ^1L_b energies with respect to the ground state of *p*-cyanophenolate alone. (b) ^1L_a and ^1L_b transition energies.

of *p*-CP^-, one can note that the $^1A_1$ (^1L_a) excited state has a non-negligible charge-transfer character: the variation of the dipole moment in the $S_0 \rightarrow {}^1A_1$ transition (1.06 au) can be reproduced by the transfer of a negative charge of about 0.10 *e* from the oxygen atom to the CN group (or 0.21 *e* from the O to the ring center); further, the presence of a charge-transfer contribution from the oxygen for the $^1A_1$ excited state of *p*-CP^- will also be confirmed by separate consideration in section 4.1 below. The $^1B_1$ (^1L_b) state shows a smaller variation of dipole moment and, moreover, is in the opposite direction compared to $^1A_1$; therefore, we do not infer any charge-transfer contribution from the oxygen atom for the $^1B_1$ state.

For the two other isomers (ortho and meta), the lowering of symmetry makes the interpretation more difficult; in particular, it would be much more difficult to establish the presence of a conical intersection (and to locate it). Note, however, that for all three isomers, as for the phenolate anion, one of the two singlets considered shows non-negligible mixing with Rydberg states (as one can see from the $\langle z^2 \rangle$ values of Table 9). As expected, there is a correlation between the Rydberg character of the state and its oscillator strength: in all cases, the singlet with lower oscillator strength is also the most diffuse one. Judging by the variations in the dipole moment on the *y* direction, it seems that the diffuse character of the state is correlated with the presence of a charge-transfer contribution. However, for the ortho and meta isomers, both S_1 and S_2 show an important diminution of μ_y with respect to the ground state, so we expect some charge transfer from the oxygen atom to the ring for both S_1 and S_2 (more accentuated for the state with some Rydberg character).

4. Acidity Calculations

4.1. Gas-Phase Proton Affinities. A convenient measure of the gas-phase acidity is the proton affinity (PA) of the anions. We have obtained PA values for phenolate and cyanophenolate anions as PA = *E*(anion) − *E*(neutral), using energies from state-to-state CASSCF calculations in order to obtain quantities comparable to the solution-phase calculations of the next two subsections. (CASPT2 energies have been disregarded in this connection also because of divergence of the wave function perturbative correction in some cases, as pointed out in section 3.3.) Our findings, together with the available experimental results, are shown in Table 10; because of convergence problems with state-to-state CASSCF calculations on S_2, only the S_0 and S_1 states have been considered. As previously indicated in section 2, ground-state RHF/cc-pVDZ-optimized geometries have been used in all the calculations discussed in the present section.

Table 10. Gas-Phase Proton Affinities and V_{min} (in eV)

	PA (S_0)			PA (S_1)		V_{min} (ArOH)		V_{min} (ArO^-)	
molecule	calc	ZPE[a]	exp	calc	exp	S_0	S_1	S_0	S_1
PhOH	15.57	15.20	15.20[b]	14.51	14.30[c]	−1.99	−1.92	−8.04	−5.39
o-CP	14.89	14.52	14.56[d]	14.43		−1.48	−1.33	−7.47	−6.33
m-CP	14.97	14.60	14.64[d]	14.08		−1.48	−1.37	−7.40	−5.76
p-CP	14.80	14.43	14.48[d]	14.03		−1.42	−1.43	−7.01	−4.70

[a] Calculated PA taking into account of the ZPE variation as indicated in the text. [b] See text. [c] Estimated from ref 46. [d] Values obtained from the relative acidity scale of ref 61, using 15.20 eV for the phenol PA.

We consider first the ground-state results. The experimental value can be deduced from the scheme

$$\mathrm{PA(PhO^-)} = \mathrm{IE(H)} + D(\mathrm{PhO{-}H}) - \mathrm{EA(PhO^\bullet}) \quad (1)$$

where IE(H) = 13.606 eV is the ionization energy of H$^\bullet$, D(PhO−H) is the dissociation energy of the PhO−H bond, and EA(PhO$^\bullet$) is the electron affinity of the phenoxyl radical. From EA(PhO$^\bullet$) = 2.253 eV (see section 3.2) and D(PhO−H) = 3.848 eV (recommended value, from the extensive compilation of literature data by Borges dos Santos and Martinho Simões[45]), one obtains PA(PhO$^-$) = 15.201 eV. Taking into account the difference in zero-point energy between the neutral and deprotonated phenol, which has been evaluated[10] at 0.37 eV for S_0, we find a PA of 15.20 eV, in very good agreement with the experimental result. For cyanophenols, we expect approximately the same variation of ZPE; in fact, the sum of the half frequencies of the stretching, in-plane bending, and out-of-plane bending vibrations of OH gives 0.328 eV for *o*-CP,[44] to be compared to 0.320 for phenol.[28] Subtracting 0.37 eV from our calculated PA, we obtain 14.52, 14.60, and 14.43 eV for *o*-, *m*-, and *p*-cyanophenolate, respectively, which are smaller than the experimental values by only 0.3% in all three cases. A decreasing value of PA corresponds to an increasing value of the acidity, and hence the gas-phase acidity scale is para > ortho > meta.

We now turn to the excited-state calculations. The experimental value of 14.30 eV for the phenolate S_1 PA shown in Table 10 has been estimated from the proton affinities of ammonia clusters,[46] knowing that the proton-transfer reaction occurs for a cluster size of six or seven ammonia molecules in S_0 and for four ammonia molecules in S_1. Using the ground-state value as a reasonable approximation for the excited-state ZPE difference between phenol and phenolate, we find 14.14 eV for the S_1 PA of phenolate, in good agreement with the experimental value. All the systems considered here are more acidic in the excited state, with decreasing acidity variations in the order phenol, *m*-CP, *p*-CP, *o*-CP (PA($S_0 - S_1$) = 1.06, 0.89, 0.77, 0.46 eV, respectively). Note, in particular, that in S_1 the acidity order of the *o*- and *m*-cyanophenols is inverted with respect to the ground state. (Note that in the above acidity order arguments, we are imagining the appropriate electronically adiabatic connection between the acid and the anion; see Figure 3.) There appear to be no gas-phase data for comparison with this prediction.

We pause to note that our excited-state proton affinities are obtained using the ground-state geometries: considering that a quite large geometry change is evidenced on going from S_0 to S_2 (^1L_a) in phenol (see section 3.1), one might expect a similar geometry change from S_0 to S_1 (^1L_a), at least for phenolate and *p*-cyanophenolate. Therefore, considering that the S_1 geometry of phenol is very similar to that of the ground state, one could expect the S_1 PA of phenolate and *p*-cyanophenolate to be overestimated. But the contribution of ΔZPE has also to be taken into account (we have used the S_0 ΔZPE in the calculation of the S_1 PA, see above), and its variation from S_0 to S_1 is much more difficult to assess. Despite these uncertainties, the good agreement with the experimental result noted above for the S_1 PA of phenolate indicates that the net consequences of these effects are not very important.

Since it has already been indicated in section 3 that the locally excited Franck−Condon S_1 state of the acid is not characterized by significant charge transfer, but that the S_1 state of the anion is, it is natural to ask if the enhanced acidity of the excited state might be more related to electronic effects in the product anion rather than in the reactant acid. Indeed, it has been shown in various ways that the differences in ground-state acidity among several substituted phenols are due mainly to effects in the phenolate anions, the effects in the corresponding phenols being of minor importance.[38,47] To show that this observation also applies to the difference between the ground- and the excited-state acidities, we report in Table 10 the calculated minimum of the electrostatic potential $V(\vec{r})$ in the vicinity of the oxygen atom (V_{min}); it has already been shown that there is a good correlation between V_{min} and ground-state pK_a values of some para-substituted phenols.[48] The potential $V(\vec{r})$ gives the interaction energy between a unit positive charge located at $\vec{r}$ and the unperturbed molecular charge distribution, and the minima of $V(\vec{r})$ are therefore the points of maximum electrostatic attraction between the (unperturbed) molecule and an approaching electrophile. The negative values of V_{min} for S_0 in Table 10 are significantly greater in magnitude for the anions than for the acids, reflecting the larger magnitude of negative charge density on the oxygen in the former case. What it is important is the relative change in V_{min} on going from S_0 to S_1; a larger relative reduction in the magnitude of V_{min} for the anion than for the acid would indicate a larger impact on the acidity increase (reduction in the magnitude of relative charge on the O) for the anion than for the acid, and vice versa. It is evident from Table 10 that from S_0 to S_1, V_{min} undergoes a much greater relative reduction in magnitude for the anions than for the neutrals; this supports the conclusion that, at least from the electrostatic point of view, the increase in S_1 acidity is largely determined by effects in the anions.[49]

4.2. Solution-Phase Transition Energies. Before proceeding to solution-phase equilibrium constants in the next subsection, we pause to consider the aqueous-phase transition energies for the acid and anionic species to help assess and calibrate our theoretical results.

The $S_0 \rightarrow S_1$ transition energies in aqueous solution are shown in Table 11, which also includes the shifts with respect to the

(45) Borges dos Santos, R. M.; Martinho Simões, J. A. *J. Phys. Chem. Ref. Data* **1998**, *27*, 707.

(46) Martrenchard-Barra, S.; Dedonder-Lardeux, C.; Jouvet, C.; Solgadi, D.; Vervloet, M.; Grégoire, G.; Dimicoli, I. *Chem. Phys. Lett.* **1999**, *310*, 173.

(47) (a) Pross, A.; Radom, L.; Taft, R. W. *J. Org. Chem.* **1980**, *45*, 818. (b) Kemister, G.; Pross, A.; Radom, L.; Taft, R. W. *J. Org. Chem.* **1980**, *45*, 1056.

(48) Haeberlein, M.; Brinck, T. *J. Phys. Chem.* **1996**, *100*, 10116.

Table 11. Phenol and Cyanophenols in Aqueous Solution: $S_0 \rightarrow S_1$ Transition Energy and Shift with Respect to the Transition Energy in the Gas Phase (eV)

	transition energy			shift		
molecule	calc	exp	exp[a]	calc	exp	exp[b]
PhOH	5.006	4.59[c]		0.025	0.00[d]	
o-CP	4.627	4.15[e]	4.18	−0.001	−0.06[f]	−0.01
m-CP	4.850	4.23[e]	4.22	−0.009		−0.04
p-CP	4.958	4.43[e]	4.40	0.027	<−0.07[g]	0.12
PhO^-	4.402	4.32[c]		0.479	0.7[h]	
o-CP^-	4.319	3.79[e]	3.85	0.157		0.25
m-CP^-	4.218	3.79[e]	3.90	0.243		0.69
p-CP^-	4.620			0.460		

[a] Absorption maxima, ref 50. [b] Estimated from Kamlet and Taft solvatochromic analysis (see text). [c] Absorption maxima, refs 41 and 62. [d] Gas-phase vertical excitation energy from ref 35. [e] Absorption maxima, ref 5. [f] Gas-phase vertical excitation energy from ref 44. [g] Estimated from gas-phase adiabatic excitation energy.[60] [h] From the estimated gas-phase transition energy of phenolate (3.5−3.65 eV, see section 3.2).

transition energies in the gas phase (a positive value indicates a blue shift on going from the gas phase to solution). As stated in section 2, full equilibrium between solute and solvent charge distribution for ground and excited states has been considered in the continuum solvation model we have used. Therefore, nonequilibrium solvation effects on the transition energies have been neglected. However, due to the very small difference between S_0 and S_1 dipole moments of phenol and cyanophenols, we expect nonequilibrium solvation effects to be negligible for the protonated species. In contrast, they could be important for the anions, since the results of section 3 indicate a much more significant charge rearrangement between S_0 and S_1.

In column 4 of Table 11, we also show our experimental values for the $S_0 \rightarrow S_1$ transition energies in the aqueous phase (absorption maxima), which are in good agreement with those of ref 5 and will be reported in detail in a forthcoming publication.[50] The shifts reported in the last column of Table 11 are obtained from our experimental solvatochromic analysis,[50] performed using the Kamlet and Taft method,[51] which makes it possible to obtain an extrapolated transition frequency corresponding to a condition where no intermolecular interactions occur and which is usually very close to the gas-phase value of the transition, at least for the neutral species. For the anions, it yields a value which can be considered as the transition energy in a weakly interacting solvent.

We consider first the protonated species. Most of the difference between our calculated transition energies and the experimental ones, which is positive and in the range 0.4−0.6 eV, is already present in our gas-phase state-to-state CASSCF calculations[52] and should not be attributed to deficiences in the description of solvation effects. In fact, as one can see from Table 11, there is a good agreement between the calculated and the experimental shifts of the $S_0 \rightarrow S_1$ transition, especially for PhOH, *o*-CP, and *m*-CP, while for *p*-CP the calculated shift has an error of about 0.1 eV. Note that the difference between calculated and experimental shifts is always positive (except for *p*-CP, considering our experimentally evaluated shift). In our PCM calculations, the dispersion−repulsion contribution to the free energy of the solute has been obtained with the semiempirical method of Floris and Tomasi,[53] which does not distinguish between ground and excited states. As S_1 is usually expected to be more polarizable than S_0, the difference between calculated and experimental shifts could come from the dispersion contribution. These issues aside, the essential point in Table 11 for the acids is that, both theoretically and experimentally, solvation effects are quite minor, consistent with the negligible charge redistribution in the $S_0 \rightarrow S_1$ transition.

For the anions, because of the important differences in the S_0 and S_1 electrostatic distributions, both nonequilibrium and dispersion−repulsion effects are expected to be much more important than in the protonated species. This is confirmed by the less good agreement (but, however, still reasonable) between calculated and experimental shifts for phenolate with respect to the protonated species (see Table 11). But these details aside, the *essential point* for the anions is that reflected by the trends rather than the precise numbers: both experimentally and theoretically for phenolate, and as (approximately) predicted experimentally and theoretically for the substituted phenolate ions, the solvent shifts for $S_0 \rightarrow S_1$ are significant, and much more pronounced than for the acid, reflecting the non-negligible charge transfer accompanying the transition in the anions.[54] Another important point, which will be discussed in the next subsection, is that the solvent shift for the $S_0 \rightarrow S_1$ transition in the anions is always positive (i.e., blue shift).

4.3. Equilibrium Constants in Solution. Since we are not dealing explicitly with the proton-accepting base partner in the present work, we need to introduce a certain measure of the acidity which is independent of that base. For this purpose, we have defined a solution-phase proton affinity PA_s of an anion, by analogy to the gas-phase PA, as

$$PA_s = G(ArO^-) - G(ArOH) \qquad (2)$$

in terms of the free energies of the solvated species. Each of these is the sum of the vacuum internal energy of the solute, $E_{vac} = \langle \Psi_0 | H_0 | \Psi_0 \rangle$, in which H_0 and Ψ_0 are the solute Hamiltonian and wave function in vacuo, respectively, and the solvation free energy ΔG_s. The latter is expressed as[14]

$$\Delta G_s = G_{IEC} + G_{el} + G_{cav} + G_{dis-rep} \qquad (3)$$

where $G_{dis-rep}$ is the dispersion−repulsion term (described in

(49) For *p*-CP, we were able to obtain V_{min} values for the S_2 state also: the results are −0.16 and −6.35 eV, respectively, for the neutral and the anion and further support our view of the inversion of states, and corresponding differences in charge-transfer character of S_1, between the acid and the anion. Note, on comparison with Table 10, that the values just cited indicate that the V_{min} diminution from S_0 to S_2 is more important for the acid than for the anion, as one should expect from the electrostatic features of the S_2 state shown in section 3. Hence, the standard view for the enhanced excited-state acidity, at least for the phenols, would, in fact, be much more suitable for the higher excited S_2 state than for the experimentally relevant S_1 state.

(50) Brenner, V.; Granucci, G.; Hynes, J. T.; Lahmani, F.; Marguet, S.; Millié, P.; Tran-Thi, T. H.; Zehnacker, A. In preparation, 2000.

(51) (a) Kamlet, M. J.; Abboud, J. L. M.; Abraham, M. H.; Taft, R. W. *J. Org. Chem.* **1983**, *48*, 2877. (b) Marcus, Y.; Kamlet, M. J.; Taft, R. W. *J. Phys. Chem.* **1988**, *92*, 3613.

(52) The $S_0 \rightarrow S_1$ gas-phase vertical transition energy used in Table 11 for phenol is 4.981 eV (obtained as the difference between the values in the second and fifth columns); it differs from the value shown in Table 2 (4.877 eV) essentially because of the different geometry: in this section we used RHF-optimized geometries, while the result shown in Table 2 is obtained at the CASSCF-optimized geometry. The other possible source of disagreement (state-to-state rather state-averaged CASSCF calculation, as in section 3) is present also for the other species shown in Table 11; it gives rise to some differences for *o*-CP and for the anions.

(53) Floris, F.; Tomasi, J. *J. Comput. Chem.* **1989**, *10*, 616.

(54) One might wonder if the gas-phase S_2 state of the anion—with its evident reduced charge-transfer character compared to the gas-phase S_1 state, which would make it more polar—could be sufficiently differentially stabilized by equilibrium solvation to cause a solvent-induced inversion compared to the gas phase. At least for the cases of phenolate and *p*-cyanophenolate, we have confirmed that this does not occur. That is to say, the S_1 state in solution is the one of L_a character, as in the gas phase.

Table 12. Acidity of Phenol and Cyanophenols in Aqueous Solution: Proton Affinities PA_s (eV), pK_a, and ΔpK_a at 298 K

	S_0		S_1		ΔpK_a ($S_0 - S_1$)	
molecule	PA_s	pK_a	PA_s	pK_a	calc	exp
PhOH	13.121	9.82[a]	12.517	4[b]	10.2	6
o-CP	12.704	6.97[c]	12.396	0.66[c]	5.2	6.3
m-CP	12.925	8.34[c]	12.293	1.89[c]	10.7	6.4
p-CP	12.844	7.74[c]	12.505	3.33[c]	5.7	4.4

[a] From ref 63. [b] From ref 62. [c] From ref 5.

Table 13. Phenol and Cyanophenols in Aqueous Solution: Computed Solvation Free Energies (ΔG_s) and Their Components at 298 K (eV)

solute	state	IEC[a]	el[b]	cav[c]	dis−rep[d]	ΔG_s
PhOH	S_0	0.0064	−0.242	0.698	−0.603	−0.141
	S_1	0.0056	−0.217	0.698	−0.603	−0.116
o-CP	S_0	0.0080	−0.293	0.797	−0.628	−0.116
	S_1	0.0087	−0.294	0.797	−0.628	−0.117
m-CP	S_0	0.0120	−0.383	0.808	−0.631	−0.194
	S_1	0.0137	−0.394	0.808	−0.631	−0.203
p-CP	S_0	0.0131	−0.396	0.808	−0.632	−0.207
	S_1	0.0125	−0.369	0.808	−0.632	−0.180
PhO^-	S_0	0.0349	−2.720	0.672	−0.580	−2.593
	S_1	0.0162	−2.222	0.672	−0.580	−2.114
o-CP^-	S_0	0.0340	−2.515	0.782	−0.605	−2.305
	S_1	0.0284	−2.352	0.782	−0.605	−2.147
m-CP^-	S_0	0.0287	−2.443	0.784	−0.607	−2.237
	S_1	0.0185	−2.190	0.784	−0.607	−1.994
p-CP^-	S_0	0.0221	−2.365	0.786	−0.608	−2.165
	S_1	0.0197	−1.902	0.786	−0.608	−1.704

[a] Contribution due to the internal energy change of the solute, see text. [b] Electrostatic interaction contribution. [c] Pierotti−Claverie cavitation energy. [d] Dispersion−repulsion contribution.

the preceding subsection), G_{cav} is the cavitation free energy, evaluated with the Pierotti−Claverie formula, G_{el} is the electrostatic contribution,[14] and

$$G_{IEC} = \langle \Psi | H_0 | \Psi \rangle - E_{vac} \tag{4}$$

is the internal energy change of the solute, where Ψ is the solute wave function in the presence of the solvent. Note that the quantity G_{IEC} has to be positive.[55]

The calculated values of PAs, eq 2, are shown in Table 12, while Table 13 gives the assorted ingredients of the solvation free energies, eq 3. Note that since these are equilibrium solvation thermodynamic properties, our full equilibrium solvation calculations for the excited states are appropriate. However, any solute geometry rearrangements after solvation of ground and excited states have been neglected.

Our results well reproduce the experimental ground-state acidity order in aqueous solution. Note, in particular, that Tables 12 and 10 show that the acidity order of *o*- and *p*-CP is inverted with respect to the gas phase; the *o*-CP is the more acidic isomer in solution. This phenomenon may involve a difference in the protonated forms; in fact *o*-CP, as described in section 3.3, forms an intramolecular hydrogen bond in the gas phase which could be expected to reduce its acidity with respect to the other isomers.

Turning to the excited-state results in Table 12, there is a less good agreement for the acidity ordering inferred from the calculated anion PA_s values and as indicated by the experimental pK^*_a values. In particular, the acidity of *o*- and *m*-CP is inverted, but at least it is correctly predicted that all the substituted phenols should be more acidic than phenol itself.

(55) Amovilli, C.; Mennucci, B. *J. Phys. Chem. B* **1997**, *101*, 1051.

The solution proton affinities can be further used to make quantitative estimates of the change in acidity for the excited compared to the ground state via $\Delta pK_a = pK_a(S_0) - pK_a(S_1)$ in the following way. In the gas phase, one has the relation

$$\Delta pK_a(\text{gas}) = \frac{1}{2.3RT}[PA(S_0) - PA(S_1)] \tag{5}$$

neglecting the difference between the entropic contribution of the ground and excited states. Note that any reference to the base cancels on the left-hand side. The same equation will be valid in solution upon substitution of PA_s for PA,

$$\Delta pK_a(\text{soln}) = \frac{1}{2.3RT}[PA_s(S_0) - PA_s(S_1)] \tag{6}$$

where, given the definition eq 2 for PA_s in terms of free energy differences, there is no approximation of ignoring entropy terms. The calculated ΔpK_a values are shown in Table 12; the agreement with the experimental results is not very good but is reasonable, considering the approximations involved (unrelaxed geometries; ZPE corrections; difficulties in calculation of the $S_0 \rightarrow S_1$ transition energy for the anions, even in gas phase; simplicity of the solvation model used).

Another useful expression for ΔpK_a(soln) is

$$\Delta pK_a(\text{soln}) = \Delta pK_a(\text{gas}) - \frac{1}{2.3RT}[\Delta\Delta G_s(ArO^-) - \Delta\Delta G_s(ArOH)] \tag{7}$$

where $\Delta\Delta G_s = \Delta G_s(S_1) - \Delta G_s(S_0)$ is the difference between the free energies of solvation of S_1 and S_0. The calculated shift of the $S_0 \rightarrow S_1$ transition reported in Table 11 also coincides (neglecting equilibrium geometry variation between ground and excited states, and also geometry rearrangements in solution) with $\Delta\Delta G_s$. One can again note that the variation of ΔG_s between S_1 and S_0 is much larger for the anions than for the neutrals, and that $\Delta\Delta G_s$ is positive for all the anions. Such behavior is connected to the charge-transfer character of the S_1 state of the anions: a more delocalized negative charge gives a less important favorable electrostatic interaction with the solvent. Hence, the phenoxide and cyanophenoxide anions have a more favorable (i.e., more negative) solvation stabilization ΔG_s in the ground than in the excited state: thus, by eq 7, the increase in acidity upon electronic excitation is less pronounced in solution than in the gas phase.[56] A similar phenomenon has been already pointed out by McMahon and Kebarle[57] in comparing the (ground-state) acidities of some substituted phenols; it appears that the increase in gas-phase acidity due to an acidifying substituent is accompanied by an unfavorable effect of the same substituent on the solvation of the ion, in hydrogen-bonding solvents.

Equation 7 can also be used in a reverse sense to infer solvation effects on ΔpK_a. Taking phenol as an example, with the experimental gas-phase ground- and excited-state PAs in Table 10, one has an experimental ΔpK_a(gas) of 15.22 (at 298 K). Inserting this value in eq 7 and using $\Delta\Delta G_s(PhOH) \simeq 0$ (see Table 11), one finds a predicted $\Delta\Delta G_s(PhO^-)$ of 0.55 eV, which is in reasonable agreement with our calculated value (0.479 eV) and with the experimental value of 0.7 eV reported in Table 11 and evaluated as the shift of the $S_0 \rightarrow S_1$ transition in phenolate. Indeed, such results support our picture, perhaps

(56) Note that this is a statement about ΔpK_a; the gas-phase ground-state acidity of an acid can be extremely weak due to the lack of solvent stabilization of the ionic product, precluding convenient spectroscopic study.

(57) McMahon, T. B.; Kebarle, P. *J. Am. Chem. Soc.* **1977**, *99*, 2222.

even more than do the results[58] shown in Table 12; a positive (and large) $\Delta\Delta G_s$ for phenolate agrees, as noted above, with the presence of a non-negligible charge-transfer character in the S_1 state of phenolate. Therefore, the S_1 state changes its nature on going from phenol to phenolate, as evidenced in the previous sections, and involving a conical intersection (section 3.2). Note that this should be, a fortiori, the case in the gas phase (see note 54). From the values shown in Table 12, we expect a similar conclusion to follow for the CP isomers.

5. Concluding Remarks

In this paper, we have undertaken a theoretical study of the ground- and excited-state acidity of phenol and cyanophenols. We first characterized the ground and the first excited singlet of the acid/base couples considered here in the gas phase. Two main results were found. First, the enhanced excited-state acidity of phenol and cyanophenols appears to be largely determined by the behavior of the deprotonated species, in contrast with, as noted in the Introduction, a standard explanation[2,3] for hydroxyarene acids, in which the S_1 increase in acidity is attributed to a charge transfer in the protonated species. Second, at least for phenol and *p*-cyanophenol, we have presented evidence for an inversion of ^1L_b and ^1L_a excited states on going from the protonated form to the anion. Our solution-phase calculations, performed using the PCM method, show the same main features found in the gas phase. For phenol and *p*-cyanophenol, two experimental solution-phase results are in agreement with the $^1L_b/^1L_a$ inversion: (a) the pattern of the oscillator strengths and (b) the excited state of the anion being less well solvated than its ground state. Such an inversion is interesting per se and in the reaction context. Our calculations indicate that the excited-state potential energy surfaces of phenol and *p*-CP are characterized by the presence of a conical intersection along the C−O axis approach of the proton, with the necessary impact of an avoided crossing in its neighborhood, i.e., along the physically relevant O−H axis direction. Such a crossing should play a key part in the dynamics of the excited-state proton-transfer process from phenol, and other acids, to water.

While our calculated solution-phase proton affinities for the anions reproduce the experimental acidity trends of both the ground- and excited-state acids as reflected in pK_a values (with the exception of one pair of cyanophenolate isomers in the excited state), our calculated differences between the ground and the excited-state pK_a of phenol and cyanophenols are only in qualitative agreement with the experimental results, with errors up to 4 pK_a units. Such errors are most probably due to the approximations involved with our solution calculations, considering the quantitative agreement of calculated gas-phase proton affinities with the experimental ones.

As we have noted in sections 1 and 3, there has been previous discussion of $^1L_b/^1L_a$ inversion between the acid reactant and the ionic products in ESPT, largely in connection with naphthol.[18] To our knowledge, the present work is the first ab initio calculation showing this inversion in the gas phase. In addition, those discussions[18a−c] make no connection to a standard view of enhanced acidity due to charge transfer from the O to the ring system in the reactant acid; in the present work, this issue has been connected to the near absence of that charge transfer in S_1 for the acid (and presence in S_2) but its presence in the anionic product in S_1 (and near absence in S_2).[64]

In future work, explicit inclusion of the proton-accepting water molecule, as well as further solvating water molecules, will be effected, and the actual dynamics of the excited-state proton-transfer reactions will be addressed. As recently suggested,[4] the latter could be more complex than is usually conceived and involve a number of steps, with a solvent-induced $^1L_b/^1L_a$ inversion in the excited acid preceding the actual proton-transfer step. In any event, in view of the clear importance of the solvent molecules in all aspects of ESPT, the provision of a complete thermodynamic and dynamic picture of ESPT certainly requires this inclusion.

Acknowledgment. The help of B. Mennucci on the PCM calculations is gratefully acknowledged. We also thank F. Lahmani and A. Zehnacker for helpful discussions. Two of the authors (T.-H.T.-T. and J.T.H.) acknowledge the support of an NSF−CNRS U.S.−France International Collaboration grant. J.T.H. acknowledges support from the U.S. NSF Grant CHE 9700419, and a Research and Creative Work Faculty Fellowship from the University of Colorado. This work was performed while G.G. was recipient of a TMR Marie Curie research training grant.

JA993730J

(58) Gao et al.[11] were able to obtain $\Delta pK_a(soln) = 8.6$ for phenol, but their $\Delta\Delta G_s(PhO^-)$ is negative (−0.12 eV), in striking disagreement with our calculated values and the experimental values.

(59) Lahmani, F.; Zehnacker, A. Private communication.

(60) Taylor, A. G.; Leutwyler, S. Unpublished data.

(61) Fujio, M.; McIver, R., Jr.; Taft, R. W. *J. Am. Chem. Soc.* **1981**, *103*, 4017.

(62) Wehry, E. L.; Rogers, L. B. *J. Am. Chem. Soc.* **1965**, *87*, 4234.

(63) Mikami, N. *Bull. Chem. Soc. Jpn.* **1995**, *68*, 683.

(64) Note added in proof: We would like to bring the reader's attention to several additional references concerned with aspects of ion stabilization in naphthol and related acids (18c, 65).

(65) (a) Agmon, N.; Huppert, D.; Masad, A.; Pines, E. *J. Phys. Chem.* **1991**, *95*, 10407. (b) Agmon, N.; Huppert, D.; Masad, A.; Pines, E. *J. Phys. Chem.* **1992**, *96*, 2020. (c) Solntsev, K. M.; Huppert, D.; Agmon, N. *J. Phys. Chem. A* **1998**, *102*, 9599. (d) Solntsev, K. M.; Huppert, D.; Agmon, N. *J. Phys. Chem. A* **1999**, *103*, 6984.